Pore-water geochemistry, JAPEX/JNOC/GSC Mallik 2L-38 gas hydrate research well

R.E. Cranston[1]

Abstract: A pore-water research program was designed to measure dissolved components in interstitial water from sediment core samples collected during the JAPEX/JNOC/GSC Mallik 2L-38 gas hydrate research-well project. Pore waters from the gas-hydrate-bearing samples had an average salinity of 8 ppt compared to 34 ppt for non-gas-hydrate-bearing samples. The difference in salinities suggests that 80–90% of the pore space in the gas-hydrate-bearing sediment was filled with gas hydrate, which dissociated during recovery. Potassium concentration was also measured in pore water, to estimate the amount of drill-mud contamination in pore-water samples, since the drill mud contained brine solution made from potassium chloride. On average, pore-water salinities were estimated to be enhanced by 2 ppt due to drill-mud contamination.

Résumé : Un programme de recherche portant sur les eaux interstitielles a été conçu dans le but de mesurer les éléments dissous dans l'eau interstitielle que renferment les échantillons carottés de sédiments prélevés dans le cadre du projet du puits de recherche sur les hydrates de gaz JAPEX/JNOC/GSC Mallik 2L-38. La salinité moyenne des eaux interstitielles était de 8 x 10^{-3} dans les échantillons renfermant des hydrates de gaz alors qu'elle était de 34 x 10^{-3} dans les échantillons sans hydrates de gaz. La différence de salinité semble indiquer que dans les sédiments renfermant des hydrates de gaz, 80 à 90 % de l'espace poral est rempli d'hydrates de gaz qui se sont dissociés au cours de la récupération. On a également mesuré la concentration de potassium contenue dans les eaux interstitielles. Ces résultats nous ont permis d'estimer l'importance de la contamination des échantillons d'eau interstitielle par la boue de forage, puisque cette boue renferme une solution saline composée de chlorure de potassium. La contamination par la boue augmente en moyenne de 2 x 10^{-3} la salinité des eaux interstitielles.

[1] Geological Survey of Canada (Atlantic), P.O. Box 1006, Dartmouth, Nova Scotia, Canada B2Y 4A2

INTRODUCTION

During the formation of gas hydrate, fresh water forms the clathrate cage. When gas hydrate forms in saline zones, the dissolved salt is not included in the structure, thus increasing the salinity of nearby pore water. When gas-hydrate-bearing sediment samples are recovered, increasing temperature and decreasing pressure allow the gas hydrate to dissociate, releasing fresh water into the pore spaces, thus reducing the salinity of the pore water. The presence of low salinities can be used to identify the existence of gas hydrate, as well as to estimate the amount of gas hydrate in the pore space. Recent work by the Ocean Drilling Program has shown that pore-water freshening of 5% represented a gas hydrate content of 5% of the pore space (Paull et al., 1996). Ginsburg and Soloviev (1998, p. 156) provided a summary of 29 gas hydrate sites where pore-water samples were freshened by an average of 20% after gas hydrate melted. Freshening was reported by Cranston (1991a), Cranston and Standing (1992), Ginsburg et al. (1993), and Cranston et al. (1994) for the Okhotsk Sea where salinities were found to decrease by 40% and gas hydrate occupied 60% of the pore space.

A salinity decrease in pore water is not necessarily due to the presence of gas hydrate. Pore waters can have low salinity due to a) minerals releasing bound water, b) ion uptake and/or release as pore water moves through clay minerals, c) influx of fresh groundwater along continental margins, and/or d) sediment burial in conditions where overlying water was fresher (Ginsburg and Soloviev, 1998, p. 155). In order to verify the presence of gas hydrate, other observations need to be made in conjunction with salinity measurements. These include a) looking for a temperature drop in core samples immediately after recovery (dissociation of gas hydrate is an endothermic process), b) fluidization of sediments as gas and water is released, and c) increasing water and gas contents in gas-hydrate-bearing samples (Ginsburg and Soloviev, 1998, p. 149).

The purpose of this pore-water program was to determine the salinity in gas-hydrate-bearing and gas-hydrate-free samples from the JAPEX/JNOC/GSC Mallik 2L-38 gas hydrate research well in an effort to estimate the amount of gas hydrate in a sediment sample. Drill mud, composed of a potassium chloride brine solution, tends to contaminate core samples, artificially increasing the salinity and thereby affecting the gas hydrate estimate. In an effort to correct for drill-mud contamination, potassium was measured and a calculation was made to correct for the amount of drill mud in each sample.

METHODS

Core subsampling

During the drilling in February and March, 1998, core sections from the Mallik 2L-38 research well were cut to lengths of 1 m and extruded into PVC (polyvinyl chloride) tubing at the drill site. The sections were sealed, labelled, and transported to Inuvik, Northwest Territories by truck. At the Inuvik Research Centre laboratory, each section was split lengthwise, subsampled, and photographed.

Field laboratory activities

Twenty pore-water samples were obtained from 109 m to 176 m in the permafrost zone. (All depths were measured from kelly bushing [8.31 m above sea level]). Twenty to thirty grams of each wet sediment subsample was centrifuged in 25 mL porous-bottomed vials fitted with 25 mm diameter glass fibre filters. Approximately 1 mL of pore water was recovered after placing the sample vial in a 50 mL centrifuge tube and centrifuging the sample for 15 min at a g-force of 1000x (IEC Centra-8 Centrifuge; 14 cm radius at 2500 rpm).

Salinity was measured using an Orion model 125 conductivity meter. A 100 µL volume of pore water was diluted with 6.5 mL of deionized water. A temperature-compensated conductivity probe was used to measure the conductivity. A calibration curve was obtained by measuring the conductivity of standard IAPSO (International Association of the Physical Sciences of the Ocean) seawater. Precision and accuracy were determined to be ±0.02 ppt (parts per thousand) salinity.

Dissolved sulphate was determined using a turbidimetric method. A 50 µL volume of sample or standard was placed in a sample cuvette. Barium chloride (50 µL of 300 mM solution) was added to precipitate the available sulphate. Four millilitres of deionized water were added to dilute the sample. The turbidity was measured using a Milton Roy Spectronic Mini-20 fitted with a turbidity attachment. A calibration curve was acquired by measuring the turbidity of various dilutions of standard IAPSO seawater. Precision and accuracy limits were estimated to be ±1 mM.

Dissolved ammonium content was determined using a colorimetric method revised from Solarzano (1969). One millilitre of deionized water was placed in a 15 mL test tube, along with 100 µL of sample or standard. A 500 µL addition of phenol-ethanol solution (0.8 g phenol dissolved in 100 mL of ethanol) was made along with 500 µL of sodium nitroprusside solution (0.075 g of sodium nitroprusside in 50 mL of deionized water). Finally, 1 mL of oxidizing solution (1 mL of sodium hypochlorite, 0.75 g trisodium citrate, and 0.04 g sodium hydroxide in 50 mL of deionized water) was added. The mixtures were shaken and left to stand for 2 h in order for the blue colour, indicative of ammonium content, to fully develop. The colour intensity was measured at 640 nm with a Brinkmann PC900 colorimeter. A calibration curve was acquired by measuring the absorbance of various ammonium chloride solutions. Precision and accuracy were determined to be ±0.2 mM.

Dissolved silica was determined by colorimetric analyses of a reduced silicomolybdate complex. This method was adapted from Strickland and Parson (1968), as described by Mann and Gieskes (1975). Five millilitres of deionized water were placed in a 15 mL test tube. A 100 µL volume of sample or standard and 1 mL of molybdate solution were allowed to stand for 15 min. Reducing solution (1 mL of metol-sulphite, oxalic acid, and sulphuric acid) was added and the mixture

Table 1. Geochemical data from the permafrost zone.

Depth (cm) From	Depth (cm) To	Water Content %ww	Salinity0 neat ppt	NH$_4^+$ mM	Silica mM	Sulphate mM	K/Sal neat ppm/ppt	Salinity2 mud-corr. ppt	Na/Sal mud-corr. ppm/ppt	Ca/Sal mud-corr. ppm/ppt	Mg/Sal mud-corr. ppm/ppt	Resistivity Ω·m	Temperature °C	Grain Size phi	Methane mud gas ppm
10993	10997	28.3	18.3	12.6	0.18	3	125	15.5	58	57	67	725	7.0	5.7	2100
11084	11086	26.0	17.5	11.1	0.15	1	188	13.1	59	46	48	1432	7.6		2100
11179	11181	24.9	10.8	11.8	0.14	1	75	9.8	62	63	87	500	7.6		2700
11284	11286	20.7	10.0	11.9	0.12							730	7.6		2700
11381	11383	23.0	1.2	5.0	0.06							1011	7.6		2700
11400		23.0	1.0	2.8	0.09	1						2125	8.7		2700
11440	11450	31.4	23.2	13.7	0.18	1	145	19.4	63	69	64	880	8.7	5.6	2700
11535	11540	26.7	16.4	13.1	0.18							950	7.6	4.9	2700
11663	11666	27.4	8.1	9.8	0.23							402		4.9	600
11724	11726	24.8	6.6	11.6	0.17							525			600
11825	11830	23.8	3.4	5.1	0.12	1	307	1.6	245	163	139	3438		4.2	800
11845		18.2	1.8	6.6	0.07							3285			800
15100		37.9	17.6	1.8	0.08	3	173	13.6	78	34	42	2680			1400
15610		38.6	24.5	3.0	0.09	5	240	17.2	71	44	33	3364			2400
17173	17175	41.2	16.5	3.6	0.06							2188		2.8	1600
17217	17220	28.0	9.5	2.4	0.04	1	233	6.1	93	42	42	2149		2.7	1600
17325	17326	34.3	38.3	2.8	0.05	3	105	35.6	38	14	20	3261		2.9	1600
17482	17483	27.8	8.0	4.1	0.03	1	264	4.6	186	59	95	2744			1600
17560	17562	21.2	5.7	2.7	0.03	1	133	4.5	1110	39	41	2361		2.3	1600
17570		21.6	2.3	1.9	0.03							2374			1600
	drill mud		61.6	1.1	0.17		568		13	2.3	0.81				
	seawater		35				11.4		306	12	35				

Salinity0 = neat pore-water salinity; **NH$_4^+$** = ammonium; **K/Sal** = ratio of potassium (ppm) to salinity (ppt); **Salinity2** = estimate of salinity corrected for drill-mud contamination; **Na/Sal** = ratio of sodium (ppm) to salinity (ppt); **Ca/Sal** = ratio of calcium (ppm) to salinity (ppt); **Mg/Sal** = ratio of magnesium (ppm) to salinity (ppt); **mud-corr** = corrected for drill-mud contamination; **%ww** = water content calculated on a wet weight basis, i.e. weight of water per unit weight of wet sediment.

was allowed to stand for 1 h. The colour absorbance was measured at 812 nm with a Brinkmann PC900 colorimeter. A calibration curve was acquired from the absorbance of various sodium fluorosilicate solutions. Precision and accuracy were determined to be ±0.2 mM.

Home-base laboratory activities

Because of program delays and scheduling, the field pore-water laboratory was closed before the gas hydrate zone was cored. When the gas hydrate zone was cored, 67 wet sediment samples were retrieved and stored at 4°C in sealed vials and plastic bags. These samples were shipped to the home-base laboratory at the Bedford Institute of Oceanography, Dartmouth, Nova Scotia. Each sediment sample was divided. The first portion was centrifuged to recover neat pore water. Approximately 1 mL of pore water was recovered from each of 27 samples, while pore water was not recovered from the other 40 samples because they were too dry.

The second portion of the 67 samples was weighed and, based on water content, the volume of pore water in each sample was calculated. Five millilitres of deionized water was added and each sample was thoroughly mixed with a vortex mixer. The 'washed' samples were then centrifuged using the same equipment and procedure discussed above.

Salinity measurements were done on the 27 'neat' and the 67 'washed' (diluted) pore-water samples. Based on the amount of 'neat' pore water that was estimated to be in each sample, a dilution factor was calculated, and the 'washed' salinity was corrected to reflect the in situ salinity.

Contamination of in situ samples can result when drill mud, containing a high concentration of potassium chloride (~50 kg KCl/m^3 of solution; Ohara et al., 1999), becomes incorporated in the sample. In order to determine the effects of the drill mud on the pore waters, flame atomic absorption analyses of the potassium content were carried out on the 67 'washed' pore-water samples, and on a 'neat' sample of fluid extracted from drill mud. In addition, dissolved sodium, calcium, and magnesium were determined by flame atomic absorption analyses. Standard analytical methods were followed using a Varian model 250+ spectrometer. Standard IAPSO seawater was used to construct calibration curves. Due to limited sample volumes and extreme variations in concentrations among the sample set, the relative precision and accuracy of the cation concentrations was determined to be ±20% of the amount present.

The sediment samples from the gas hydrate zone were stored for six weeks prior to arriving at the home-base laboratory. As a result of dehydration, exposure to oxygen, and exposure to the washing procedure, sample quality had decreased. As a result, analyses of ammonium, sulphate, and silicate were not completed on samples from the gas hydrate zone.

RESULTS AND DISCUSSION

Permafrost section

Sediments in the upper 640 m at the Mallik 2L-38 well were within the ice-bearing permafrost interval (Dallimore et al., 1999). A total of 13.7 m of core was recovered between 109 m and 176 m downhole. Pore-water samples were taken from 20 intervals. Immediate analyses were done for salinity, ammonium, silica, and sulphate. Samples were stored at 4°C and returned to the home-base laboratory for major cation analyses. These results are available in Table 1, along with auxiliary

data (water content, core temperature, grain size, mud-gas methane, and resistivity log) for the same intervals, selected from data sets provided by other researchers. There was insufficient pore-water volume to do all analyses. Pore-water results for drill-mud pore fluid and standard seawater are included in the table.

Pore-water contamination from drill mud was discussed above. The pore-water sample was a mixture of natural pore water and drill mud. A calculation was made to estimate what portion of the salinity of the sample was due to drill-mud pore fluid, based on the salinity and potassium content of pore-water samples and of the drill mud, using the following equations:

$$f = S_o \cdot ((K/S)_o - (K/S)_{sw}) / (S_m \cdot ((K/S)_m - (K/S)_{sw})) \quad (1)$$

$$S_2 = (S_o - (S_m \cdot f))/(1 - f) \quad (2)$$

where f is the fraction of the mixture due to drill mud, S is salinity, K is potassium content, and subscript 'o' refers to observed in sample, subscript 'm' refers to observed in drill mud, subscript 'sw' means in sea water, and subscript '2' indicates corrected for drill mud. An assumption was made that natural pore water had a potassium/salinity ratio similar to that of seawater, a conclusion that is supported later in this discussion. The estimate of salinity corrected for drill-mud contamination (S_2) is listed as 'salinity2' in the tables.

The drill mud was depleted in sodium, calcium, and magnesium relative to seawater and as drill-mud pore water was added to neat pore water, the concentrations of these three cations were diluted. As a result, a correction for the cation/salinity ratios was done using the following equation:

$$(cation/S)_2 = ((cation/S)_o - (cation/S)_m \cdot f) / (1-f) \quad (3)$$

A Pearson correlation coefficient matrix (Table 2) was produced from the data in Table 1. Table 2 contains 'r' (correlation coefficient), 'n' (number of samples), and 'p' (the significance of the correlation, i.e. the probability that the observed correlation is due to random, unrelated events). Significant correlation coefficients ($p < 0.001$) are highlighted in bold font. A number of variables correlate to a significant degree (e.g. ammonium, silica, and the mean phi grain size decrease with depth down core; water content correlates with the neat pore-water salinity (salinity0), etc.). The sparse sampling resolution, the lack of sufficient pore water and the high variability in water content, grain size, and salinity throws into doubt the usefulness of further discussion of these results.

Gas hydrate section

The gas hydrate section was cored from 886 m to 952 m downhole, where 37.3 m of core was recovered. Sediment subsamples were sealed in containers and stored for shipment to the home-base laboratory. Salinity and cation results are available in Table 3, along with auxiliary data provided by other researchers (water content, core temperature, grain size, mud-gas methane, and resistivity log).

Neat pore-water samples were successfully recovered from 27 of the 67 samples (Table 3). The other 40 samples did not provide sufficient pore water to measure salinity. A second portion of each of the 67 samples was processed by adding 5 mL of deionized water in an effort to wash pore water from the wet sediment and obtain a diluted pore-water sample.

Figure 1 contains the salinity measured for the 27 neat pore-water samples (listed as 'salinity0' in Table 3) plotted with the 'wash-corrected' salinities ('salinity1' in Table 3) for the same 27 samples. The washed salinity values were corrected for dilution, based on the water content and subsample weight for the wet sediment samples. The highly significant correlation coefficient of 0.88 ($p < 0.001$) and a regression slope of 0.97 suggests good agreement between the two sets of salinity values. A 1:1 line is included in Figure 1. The wash-corrected salinities were on average 4% less than neat pore-water salinities. It is concluded that the washing procedure was a useful approach to provide salinity values for samples where neat pore water could not be recovered.

The deionized water wash procedure has been used elsewhere in cases where insufficient pore water was available for routine extraction (Cranston, 1991b). Calcium values for washed samples were on average 5% below values for neat samples; magnesium results for washed samples were 11% less than those for neat samples. Within the sampling and analytical error, it is concluded that the cation analyses for the washed samples do provide useful information. Due to insufficient sample volume, cation analyses were not done on neat pore-water samples.
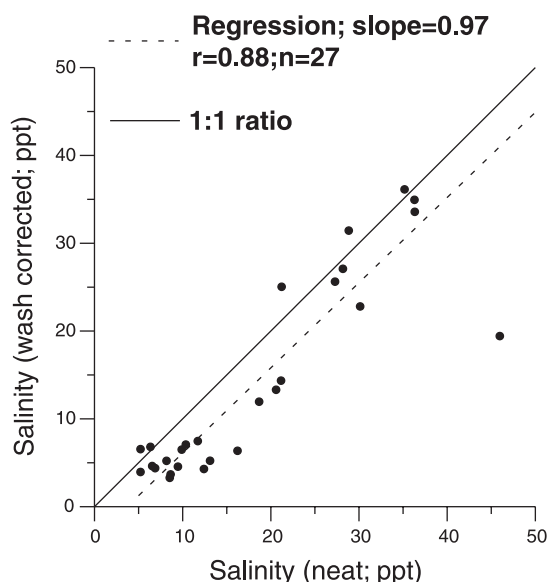
Figure 1. Wash-corrected salinity data versus neat pore-water salinity data.

Table 2. Correlation coefficients for data from the permafrost zone.

Each cell lists three values: r (correlation coefficient) / n (number of samples) / p (significance). Bolded correlation coefficients are significant at p<0.001.

	Depth	Water	Salinity0	NH_4^+	Silica	Sulphate	K/Sal	Salinity2	Na/Sal	Ca/Sal	Mg/Sal	Resistivity	Temp.	Grain size	Methane
Depth	*r / n / p*	0.39 20 0.044	0.20 20 0.197	**-0.76** 20 0.000	**-0.77** 20 0.000	0.21 12 0.254	0.18 11 0.298	0.04 11 0.454	0.38 11 0.125	-0.48 11 0.066	-0.45 11 0.084	0.60 20 0.003	0.60 8 0.057	**-0.96** 9 0.000	-0.24 20 0.158
Water	0.39 20 0.044		**0.72** 20 0.000	-0.22 20 0.171	-0.02 20 0.461	0.81 12 0.001	0.01 11 0.494	0.62 11 0.021	-0.54 11 0.042	-0.42 11 0.097	-0.51 11 0.054	0.22 20 0.174	0.15 8 0.364	-0.12 9 0.376	0.03 20 0.443
Salinity0	0.20 20 0.197	0.72 20 0.000		0.11 20 0.318	0.14 20 0.279	0.63 12 0.014	-0.43 11 0.095	**0.99** 11 0.000	-0.47 11 0.073	-0.55 11 0.040	-0.64 11 0.017	0.10 20 0.336	-0.12 8 0.388	0.06 9 0.438	0.21 20 0.187
NH_4^+	**-0.76** 20 0.000	-0.22 20 0.171	0.11 20 0.318		**0.85** 20 0.000	-0.22 12 0.244	-0.41 11 0.103	0.09 11 0.397	-0.31 11 0.173	0.20 11 0.281	0.27 11 0.211	**-0.78** 20 0.000	-0.35 8 0.200	**0.95** 9 0.000	0.25 20 0.147
Silica	**-0.77** 20 0.000	-0.02 20 0.461	0.14 20 0.279	**0.85** 20 0.000		0.00 12 0.495	-0.26 11 0.220	0.14 11 0.341	-0.43 11 0.091	0.34 11 0.154	0.28 11 0.202	**-0.69** 20 0.000	-0.17 8 0.347	**0.93** 9 0.000	0.04 20 0.437
Sulphate	0.21 12 0.254	0.81 12 0.001	0.63 12 0.014	-0.22 12 0.244	0.00 12 0.495		-0.04 11 0.451	0.53 11 0.045	-0.29 11 0.194	-0.35 11 0.140	-0.48 11 0.067	0.35 12 0.130	-0.68 5 0.102	0.21 6 0.347	0.04 12 0.447
K/Sal	0.18 11 0.298	0.01 11 0.494	-0.43 11 0.095	-0.41 11 0.103	-0.26 11 0.220	-0.04 11 0.451		-0.52 11 0.051	-0.06 11 0.436	0.54 11 0.042	0.44 11 0.088	0.60 11 0.025	0.18 4 0.412	-0.06 6 0.457	-0.55 11 0.041
Salinity2	0.04 11 0.450	0.62 11 0.021	**0.99** 11 0.000	0.09 11 0.397	0.14 11 0.341	0.54 11 0.045	-0.52 11 0.051		-0.42 11 0.100	-0.54 11 0.045	-0.61 11 0.024	0.02 11 0.471	0.56 4 0.220	0.12 6 0.412	0.32 11 0.170
Na/Sal	0.38 11 0.125	-0.54 11 0.042	-0.47 11 0.073	-0.31 11 0.173	-0.43 11 0.091	-0.29 11 0.194	-0.06 11 0.436	-0.42 11 0.099		0.00 11 0.495	-0.03 11 0.462	0.16 11 0.320	0.84 4 0.080	-0.52 6 0.144	-0.29 11 0.197
Ca/Sal	-0.48 11 0.066	-0.42 11 0.097	-0.55 11 0.040	0.20 11 0.281	0.34 11 0.154	-0.35 11 0.140	0.54 11 0.042	-0.54 11 0.045	0.00 11 0.495		**0.91** 11 0.000	0.10 11 0.387	0.59 4 0.205	0.36 6 0.238	-0.34 11 0.150
Mg/Sal	-0.45 11 0.084	-0.51 11 0.054	-0.64 11 0.017	0.27 11 0.211	0.28 11 0.203	-0.48 11 0.067	0.44 11 0.088	-0.61 11 0.024	-0.03 11 0.462	**0.91** 11 0.000		-0.05 11 0.441	-0.09 4 0.455	0.44 6 0.194	-0.27 11 0.209
Resistivity	0.60 20 0.003	0.22 20 0.174	0.10 20 0.336	**-0.78** 20 0.000	**-0.69** 20 0.000	0.35 12 0.130	0.60 11 0.025	0.02 11 0.471	0.16 11 0.320	0.10 11 0.387	-0.05 11 0.441		0.56 8 0.073	-0.70 9 0.017	-0.31 20 0.089
Temp.	0.60 8 0.057	0.15 8 0.364	-0.12 8 0.388	-0.35 8 0.200	-0.17 8 0.347	-0.68 5 0.102	0.18 4 0.412	0.56 4 0.220	0.84 4 0.080	0.59 4 0.205	-0.09 4 0.455	0.56 8 0.073		0.05 3 0.483	0.52 8 0.093
Grain size	**-0.96** 9 0.000	-0.12 9 0.376	0.06 9 0.438	**0.95** 9 0.000	**0.93** 9 0.000	0.21 6 0.347	-0.06 6 0.457	0.12 6 0.412	-0.52 6 0.144	0.36 6 0.238	0.44 6 0.194	-0.70 9 0.017	0.05 3 0.483		0.33 9 0.196
Methane	-0.24 20 0.158	0.03 20 0.443	0.21 20 0.187	0.25 20 0.147	0.04 20 0.437	0.04 12 0.447	-0.55 11 0.041	0.32 11 0.170	-0.29 11 0.197	-0.34 11 0.150	-0.27 11 0.209	-0.31 20 0.089	0.52 8 0.093	0.33 9 0.196	

Water = water content; **Salinity0** = neat pore water salinity; **NH_4^+** = ammonium dissolved; **K/Sal** = ratio of potassium (ppm) to salinity (ppt); **Salinity2** = estimate of salinity corrected for drill-mud contamination; **Na/Sal** = ratio of sodium (ppm) to salinity (ppt); **Ca/Sal** = ratio of calcium (ppm) to salinity (ppt); **Mg/Sal** = ratio of magnesium (ppm) to salinity (ppt); **Resistivity** = electrical resistivity log data; **Temp.** = core temperature; **Methane** = mud-gas methane; r = correlation coefficient; n = number of samples; p = the significance of correlation; the probability that the observed correlation is due to random, unrelated events.

Bolded correlation coefficients are significant at p<0.001.

Units:
depth (cm); water content (%); Salinity0 (ppt); NH_4^+ (mM); Silica (mM); Sulphate (mM); K/Sal (ppm/ppt); Salinity2 (ppt); Na/Sal (ppm/ppt); Ca/Sal (ppm/ppt); Mg/Sal (ppm/ppt); Resistivity ($\Omega \cdot$m); Temperature (°C); Grain size (phi units); Methane (ppm).

Table 3. Geochemical data from the gas hydrate zone.

Depth (cm) From	Depth (cm) To	Water Content %ww	Salinity0 neat ppt	Salinity1 wash-corr. ppt	K/Sal wash-soln ppm/ppt	Salinity2 mud-corr. ppt	Na/Sal mud-corr. ppm/ppt	Ca/Sal mud-corr. ppm/ppt	Mg/Sal mud-corr. ppm/ppt	Resistivity Ω·m	Temp. °C	Grain size phi	Methane mud gas ppm	Gas hydrate present notes
88666	88668	16.5		27.3	51	26.2	166	8.8	36.4	6.2	0.0		15500	0
88669	88670	16.5		32.9	85	30.7	284	9.1	37.0	6.2	0.0		15500	0
89042	89044	13.9		36.8	75	35.0	301	7.9	37.5	4.7	0.3		9123	0
89045	89047	13.9		23.4	20	23.2	226	4.6	30.8	4.6	0.3	6.1	9123	0
89090	89092	15.4	21.2	25.0	25	24.7	237	13.2	43.1	4.0	0.4		9174	0
89090	89092	15.4	28.2	27.1	61	25.7	192	10.3	41.7	4.0	0.4		9174	0
89090	89092	15.4	36.3	34.9	125	31.4	181	10.8	37.9	4.0	0.4	4.9	9174	0
89200	89202	15.0		27.5	13	27.4	273	11.3	48.4	5.0	0.6	4.9	8988	0
89200	89202	15.0		27.6	12	27.6	269	9.9	45.9	5.0	0.6	4.9	8988	0
89200	89202	15.0		30.2	25	29.8	266	14.6	46.3	5.0	0.6	4.9	8988	0
89245	89247	11.2		34.4	37	33.7	294	6.8	37.7	3.4			8988	0
89245	89247	11.2		35.2	64	33.7	283	7.3	38.2	3.4			8988	0
89245	89247	11.2		34.1	82	32.0	275	8.0	38.5	3.4			8988	0
89319	89321	13.8		34.1	79	32.1	197	11.7	39.4	5.3		4.7	8785	0
89319	89321	13.8		26.7	29	26.2	238	8.6	39.6	5.3		4.7	8785	0
89319	89321	13.8		26.6	16	26.5	286	7.6	37.1	5.3		4.7	8785	0
89655	89660	16.7		35.7	110	32.7	315	10.7	39.3	6.8	0.6		16600	0
89700	89702	14.6	35.2	36.1	100	33.5	252	12.3	38.9	4.1	0.6	5.2	125000	0
89752	89754	13.3		50.6	177	47.0	245	11.0	36.1	27.0	0.6	5.6	125000	0
89815	89816	14.6	10.4	7.1	227	4.5	218	10.5	50.7	46.0	-2.5	1.9	103000	1
89845	89847	18.0	5.2	4.0	43	3.7	265	9.3	64.4	60.0	-2.5	2.0	103000	1
90012	90016	16.8	5.2	6.6	53	6.1	231	12.8	72.0	12.0	-2.0	1.5	5300	1
90052	90054	15.0		40.2	120	37.1	251	8.3	36.5	14.0		4.3	5300	0
90220	90222	14.0		32.0	41	31.2	373	10.1	41.3	29.0	0.6	4.5	22600	0
90262	90264	14.0	30.1	22.8	224	16.4	143	14.2	47.7	27.0	0.9	2.3	121000	1
90262	90264	14.0	27.3	25.6	220	19.0	150	15.5	52.2	27.0	0.9	2.3	121000	1
90262	90264	14.0	28.8	31.4	201	25.1	145	19.4	55.4	27.0	0.9	2.3	121000	1
90346	90348	16.0	9.9	6.5	70	5.9	420	7.0	64.0	27.0	1.3	2.7	121000	1
90383	90385	15.4		43.5	75	41.9	253	12.7	40.6	15.0	1.3	6.7	121000	0
90387	90389	15.4		56.3	162	54.6	157	11.5	35.7	14.0	1.3		121000	0
90387	90389	15.4		53.2	169	50.5	177	10.9	37.3	14.0	1.3		121000	0
90450	90452	23.5	16.2	6.4	225	4.1	216	7.8	43.9	13.0	-1.7	2.8	121000	1
90548	90550	18.7	13.1	5.2	271	2.9	186	4.8	36.5	95.0	-1.0		118000	1
90577	90580	15.7	6.3	6.8	72	6.1	361	6.5	62.6	55.0	-1.5		108000	1
90660	90662	15.5		60.8	136	60.6	139	11.4	39.7	8.0	2.2	6.1	108000	0
90662	90664	15.5		53.2	112	51.7	239	13.5	45.6	8.0	2.2		108000	0
90662	90664	15.5		48.9	102	47.0	210	13.3	45.6	8.0	2.2		108000	0
91269	91271	16.5	21.2	14.4	198	10.4	153	19.3	62.8	14.0	-1.4	3.4	125000	1
91269	91271	16.5	18.7	12.0	70	10.9	201	22.2	70.0	14.0	-1.4		125000	1
91269	91271	16.5	20.6	13.3	199	9.5	142	22.8	63.5	14.0	-1.4		125000	1
91957	91959	15.1	11.7	7.5	128	6.1	189	24.6	77.0	29.0	-1.8	2.9	120000	1
92008	92010	16.6	9.5	4.6	119	3.7	275	15.6	65.2	25.0	-1.7		102000	1
92034	92036	15.0	6.9	4.4	106	3.7	210	13.6	75.5	35.0	-1.0		102000	1
92034	92036	15.0	6.5	4.6	103	3.9	202	15.7	71.3	35.0	-1.0		102000	1
92034	92036	15.0	8.2	5.2	184	3.7	164	14.1	50.5	35.0	-1.0	2.9	102000	1
92130	92132	21.4	8.5	3.3	91	2.8	235	12.0	68.3	13.0	-1.2	2.7	119000	1
92130	92132	21.4	46.0	19.4	296	11.3	100	19.7	20.9	13.0	-1.2	2.7	119000	1
92130	92132	21.4	12.4	4.3	142	3.3	203	14.0	47.2	13.0	-1.2	2.7	119000	1
92233	92236	18.5	8.6	3.7	29	3.6	328	12.2	77.5	9.0			114000	1
92730	92732	14.6	36.3	33.6	103	30.8	330	11.8	36.6	3.0	4.8	6.8	6850	0
92802	92804	14.6		43.4	24	43.1	244	10.0	42.3	3.0	4.8	5.7	6850	Gas
92853		15.0		42.6	120	39.6	246	11.2	38.1	4.0			6750	0
93605	93608	13.6		37.4	107	34.6	248	6.5	34.7	6.0		6.3	4800	0
93770	93773	14.6		31.1	103	28.3	311	8.0	36.8	4.0	6.0		3760	0
93870	93873	12.1		31.5	142	27.4	318	6.9	40.6	8.0	5.5	6.0	3400	0
94370	94372	25.3		50.6	97	49.0	193	10.8	37.3	8.0			4500	0
94370	94372	25.3		34.2	126	30.6	251	7.8	36.7	8.0			4500	0
94370	94372	25.3		51.4	139	49.0	206	9.5	40.0	8.0			4500	0
94398	94401	16.2		26.5	116	23.4	332	5.2	33.1	7.0	2.5		4500	0
94435	94439	14.4		29.3	98	26.7	307	3.8	34.3	7.0	2.5	6.5	4500	0
94502	94505	13.8		40.6	111	37.8	305	5.6	30.4	8.0	2.5	6.7	3500	0
94600	94603	12.0		26.9	49	25.9	378	4.2	33.2	6.0	2.0	6.3	3200	0
94700	94703	15.1		30.5	107	27.6	379	8.8	37.6	7.0	2.0		3200	0
94800	94803	12.8		35.8	138	31.9	282	6.9	37.0	7.0	2.9	6.4	3500	0
94897	94900	14.0		34.5	129	30.9	257	6.9	36.5	6.0	2.9		3300	0
95000	95003	13.1		42.0	109	39.4	248	7.5	33.7	6.0	2.1		2900	0
95110	95111	14.9		24.6	35	23.9	312	5.9	36.8	7.0	1.4	6.3	9600	0
drill mud			61.6		568		13	2.3	0.81					
seawater			35.0		11.4		306	12.0	35					

Salinity0 = neat pore water salinity; **Salinity1** = salinity of pore water washed from sample with deionized water and corrected for dilution; **K/Sal** = ratio of potassium (ppm) to salinity (ppt); **Salinity2** = estimate of salinity corrected for drill-mud contamination; **Na/Sal** = ratio of sodium (ppm) to salinity (ppt); **Ca/Sal** = ratio of calcium (ppm) to salinity (ppt); **Mg/Sal** = ratio of magnesium (ppm) to salinity (ppt); **wash-corr.** = pore water was washed from sample with deionized water and concentrations were corrected for dilution; **wash-soln** = pore water washed from sample with deionized water; **mud-corr** = corrected for drill-mud contamination; **%ww** = water content calculated on a wet weight basis, i.e. weight of water per unit weight of wet sediment.

Shaded areas refer to variables that indicate the presence of gas hydrate; where Salinity2 <20 ppt, Mg/Sal > 50 ppm/ppt, Resistivity > 20 Ω·m, Temperature < 0°C, Grain size mean phi < 4, Methane > 100 000 ppm.

Table 4. Comparing means for non-gas-hydrate-bearing and gas-hydrate-bearing samples.

	Non-gas-hydrate-bearing			Gas-hydrate-bearing			
	mean	SD	n	mean	SD	n	p
Water (%ww)	15.1	3.1	45	17.0	2.7	22	0.017
Salinity0 (ppt)	31.4	6.6	5	15.1	10.3	22	0.003
Salinity1 (ppt)	36.5	9.4	45	10.0	8.0	22	**0.000**
K/Sal (ppm/ppt)	88	45	45	149	79	22	**0.000**
Salinity2 (ppt)	34.5	9.3	45	7.6	5.9	22	**0.000**
Na/Sal (ppm/ppt)	261	57	45	215	77	22	0.008
Ca/Sal (ppm/ppt)	9.2	2.7	45	14.2	5.4	22	**0.000**
Mg/Sal (ppm/ppt)	38	4	45	59	14	22	**0.000**
Resistivity ($\Omega \cdot$m)	7	5	45	29	20	22	**0.000**
Temp. (°C)	1.9	1.8	34	-1.0	1.1	21	**0.000**
Grain size (phi)	5.6	0.8	22	2.5	0.5	14	**0.000**
Methane (ppm)	27 000	43 000	45	110 000	25 000	22	**0.000**

Water = water content; **Salinity0** = neat pore-water salinity; **Salinity1** = salinity of pore water washed from sample with deionized water and corrected for dilution; **K/Sal** = ratio of potassium (ppm) to salinity (ppt); **Salinity2** = estimate of salinity corrected for drill-mud contamination; **Na/Sal** = ratio of sodium (ppm) to salinity (ppt); **Ca/Sal** = ratio of calcium (ppm) to salinity (ppt); **Mg/Sal** = ratio of magnesium (ppm) to salinity (ppt); **Grain size** = average sediment particle size; **%ww** = water content calculated on a wet weight basis, i.e. weight of water per unit weight of wet sediment; **Temp.** = core temperature; **Methane** = mud-gas methane

Bolded probabilities indicate variables with significantly different means for non-gas-hydrate-bearing samples and for gas-hydrate-bearing samples.

Pore-water results for the cations K^+, Na^+, Ca^{+2}, and Mg^{+2} are included as salinity ratios in Table 3. Potassium/salinity values are based on analyses of the washed pore-water samples. The cation/salinity ratios for the remaining three cations are based on analyses of the washed pore-water samples which were then corrected for drill mud contamination.

A third salinity value in Table 3 (salinity2) is calculated to be the in situ concentration after correcting for drill mud contamination.

Gas hydrate identification

In order to compare samples with and without gas hydrate, a procedure was devised to separate the samples into two groups. Gas hydrate was observed in a number of the core sections and was suspected to occur in a number of other core sections. In addition to the visual identification of gas hydrate, negative core temperatures due to gas hydrate dissociating, high methane concentrations, and coarse-grained sediment sections appeared to correspond to gas-hydrate-bearing sediment (Collett et al., 1999; Dallimore et al., 1999; Jenner et al., 1999). Resistivity logs often showed increased measurements in gas hydrate zones (Collett et al., 1999), and low pore-water salinities can be used to indicate that gas hydrate, composed of low-salinity water, had dissociated during sample recovery (Ginsburg and Soloviev, 1998, p. 156).

Using the visual identification of gas hydrate as the starting point (Jenner et al., 1999), gas hydrate had been noted or suspected when core temperatures were negative (<0°C) (Wright et al., 1999), when mud-gas methane concentrations were high (>10% v/v; gas concentration units, based on the volume of gas at standard temperature and pressure, divided by the volume of the sample), when sediment particles were relatively coarse (mean phi<4), when resistivity was high (>20 $\Omega \cdot$m) and when pore-water salinities were low (<20 ppt). In addition to these variables, it was apparent that gas-hydrate-bearing sediments provided pore water with high magnesium/salinity ratios (>50 ppm/ppt). Using these variables as gas hydrate indicators, each subsample was rated by identifying how many of the six gas hydrate indicators occurred in that sample. Variable results in Table 3 are shaded where the value fits the model used to predict the occurrence of gas hydrate. In cases where three or more of the six indicator variables suggested the presence of gas hydrate, the final column in Table 3 was given a value of '1' to indicate that this sample had contained gas hydrate. Of 67 samples, 22 were given this status.

Comparing means

Based on the gas hydrate 'rating' value discussed above, the data in Table 3 were divided into gas-hydrate-bearing and non-gas-hydrate-bearing groups. A t-test was applied to the means calculated for the two groups. The comparative mean, standard deviation, and number of observations for each variable are reported in Table 4. The probability that the means for the two groups are from same sample variable population is reported in the last column of Table 4. As suspected from other studies of gas hydrate (e.g. Ginsburg and Soloviev, 1998, p. 149) salinity and core temperature were significantly lower in gas-hydrate-bearing samples, while resistivity, grain size, and methane concentrations were significantly higher in samples containing gas hydrate. Calcium/salinity and magnesium/salinity ratios also appeared to be higher in gas-hydrate-bearing samples. Sodium/salinity and water content means were not significantly different for the two groups.

Correlation coefficients for variables in the gas hydrate section

Table 5 is a Pearson correlation matrix for the data in Table 3. The table lists values of 'r' (correlation coefficient), 'n' (number of samples), and 'p' (the significance of the correlation) as was described for Table 2. Temperature tends to increase with depth because of the natural geothermal gradient. The three salinity values correlate positively with each other, and with temperature and mean phi grain size. The mud-corrected salinity results correlate negatively with magnesium/salinity, resistivity, and mud-gas methane concentration. The new parameter 'gas hydrate', based on the arbitrary assignment of a '1' when it appeared that gas hydrate was

Table 5. Correlation coefficients for data from the gas hydrate zone.

		Depth	Water	Salinity0	Salinity1	K/Sal	Salinity2	Na/Sal	Ca/Sal	Mg/Sal	Resistivity	Temp.	Grain size	Methane	Gas hydrate
Depth	r n p		0.20 67 0.054	-0.20 27 0.157	0.07 67 0.297	0.15 67 0.108	0.04 67 0.362	0.23 67 0.031	-0.18 67 0.066	-0.12 67 0.167	-0.12 67 0.164	**0.49** 55 0.000	0.38 36 0.012	-0.21 67 0.046	-0.07 67 0.295
Water		0.20 67 0.054		-0.13 27 0.262	-0.17 67 0.078	0.25 67 0.019	-0.18 67 0.072	-0.26 67 0.016	0.16 67 0.102	0.12 67 0.163	0.12 67 0.175	**-0.53** 55 0.000	-0.51 36 0.001	0.21 67 0.040	0.29 67 0.008
Salinity0		-0.20 27 0.157	-0.13 27 0.262		**0.88** 27 0.000	0.37 27 0.028	**0.80** 27 0.000	-0.40 27 0.020	0.23 27 0.121	**-0.74** 27 0.000	-0.46 27 0.008	0.59 26 0.001	0.56 17 0.009	-0.20 27 0.156	-0.56 27 0.001
Salinity1		0.07 67 0.297	-0.17 67 0.078	**0.88** 27 0.000		-0.07 67 0.283	**0.99** 67 0.000	-0.02 67 0.419	-0.24 67 0.023	**-0.67** 67 0.000	**-0.51** 67 0.000	**0.65** 55 0.000	**0.74** 36 0.000	-0.36 67 0.002	**-0.81** 67 0.000
K/Sal		0.15 67 0.108	0.25 67 0.019	0.37 27 0.028	-0.07 67 0.283		-0.16 67 0.102	**-0.55** 67 0.000	0.32 67 0.005	-0.06 67 0.312	**0.41** 67 0.000	-0.18 55 0.093	-0.43 36 0.004	**0.53** 67 0.000	**0.45** 67 0.000
Salinity2		0.04 67 0.362	-0.18 67 0.072	**0.81** 27 0.000	**0.99** 67 0.000	-0.16 67 0.102		0.01 67 0.458	-0.27 67 0.013	**-0.64** 67 0.000	**-0.52** 67 0.000	**0.64** 55 0.000	**0.77** 36 0.000	-0.37 67 0.000	**-0.84** 67 0.000
Na/Sal		0.23 67 0.031	-0.26 67 0.016	-0.40 27 0.020	-0.02 67 0.419	**-0.55** 67 0.000	0.01 67 0.458		**-0.58** 67 0.000	-0.09 67 0.244	-0.14 67 0.134	0.36 55 0.004	0.45 36 0.003	**-0.44** 67 0.000	-0.32 67 0.004
Ca/Sal		-0.19 67 0.066	0.16 67 0.102	0.23 27 0.121	-0.24 67 0.023	0.32 67 0.005	-0.27 67 0.013	**-0.58** 67 0.000		**0.56** 67 0.000	0.10 67 0.215	**-0.44** 55 0.000	**-0.54** 36 0.000	**0.58** 67 0.000	**0.54** 67 0.000
Mg/Sal		-0.12 67 0.167	0.12 67 0.163	**-0.74** 27 0.000	**-0.67** 67 0.000	-0.06 67 0.312	**-0.64** 67 0.000	-0.09 67 0.244	**0.56** 67 0.000		**0.39** 67 0.000	**-0.56** 55 0.000	**-0.67** 36 0.000	**0.53** 67 0.000	**0.75** 67 0.000
Resistivity		-0.12 67 0.164	0.12 67 0.175	-0.46 27 0.008	**-0.51** 67 0.000	**0.41** 67 0.000	**-0.52** 67 0.000	-0.14 67 0.134	0.10 67 0.215	**0.39** 67 0.000		**-0.49** 55 0.000	**-0.64** 36 0.000	**0.55** 67 0.000	**0.64** 67 0.000
Temp.		**0.49** 55 0.000	**-0.53** 55 0.000	0.59 26 0.001	**0.65** 55 0.000	-0.18 55 0.093	**0.64** 55 0.000	0.36 55 0.004	**-0.44** 55 0.000	**-0.56** 55 0.000	**-0.49** 55 0.000		0.75 32 0.000	**-0.53** 55 0.000	**-0.68** 55 0.000
Grain size		0.38 36 0.012	-0.51 36 0.001	0.56 17 0.009	**0.74** 36 0.000	-0.43 36 0.004	**0.77** 36 0.000	0.45 36 0.003	**-0.54** 36 0.000	**-0.67** 36 0.000	**-0.64** 36 0.000	0.75 32 0.000		**-0.58** 36 0.000	**-0.91** 36 0.000
Methane		-0.21 67 0.046	0.21 67 0.040	-0.20 27 0.156	-0.36 67 0.002	**0.53** 67 0.000	-0.38 67 0.000	-0.44 67 0.000	**0.58** 67 0.000	**0.53** 67 0.000	**0.55** 67 0.000	-0.53 55 0.000	-0.58 36 0.000		**0.72** 67 0.000
Gas hydrate		-0.07 67 0.295	0.29 67 0.008	-0.56 27 0.001	**-0.81** 67 0.000	**0.45** 67 0.000	**-0.84** 67 0.000	-0.32 67 0.004	**0.54** 67 0.000	**0.75** 67 0.000	**0.64** 67 0.000	**0.75** 55 0.000	**-0.68** 55 0.000	**0.72** 67 0.000	

Depth = depth downcore; **Water** = Water content of wet sediment; **Salinity0** = neat pore-water salinity; **Salinity1** = salinity of pore water washed from sample with deionized water and corrected for dilution; **K/Sal** = ratio of potassium (ppm) to salinity (ppt); **Salinity2** = estimate of salinity corrected for drill-mud contamination; **Na/Sal** = ratio of sodium (ppm) to salinity (ppt); **Ca/Sal** = ratio of calcium (ppm) to salinity (ppt); **Mg/Sal** = ratio of magnesium (ppm) to salinity (ppt); **Resistivity** = electrical resistivity log data; **Temp.** = core temperature; **Grain size** = average sediment particle size; r = correlation coefficient; n = number of samples; p = the significance of correlation; the probability that the observed correlation is due to random, unrelated events.

Bolded correlation coefficients are significant at p<0.001.

Units:
depth (cm); water content (%); Salinity0 (ppt); Salinity1 (ppt); K/Sal (ppm/ppt); Salinity2 (ppt); Na/Sal (ppm/ppt); Ca/Sal (ppm/ppt); Mg/Sal (ppm/ppt); Resistivity (Ω·m); Temperature (°C); Grain size (phi units); Methane (ppm).

present, tends to have a very strong negative correlation with salinity, core temperature, and mean phi grain size, while correlating strongly with calcium and magnesium salinity ratios, resistivity, and methane concentration.

Similarities of pore water to seawater

The average salinity for the 45 pore-water samples that a) did not contain gas hydrate and b) were corrected for drill-mud content, was 34.5 ppt (Table 4), similar to normal seawater (35 ppt). Cation concentrations for sodium, calcium, and magnesium, corrected for drill mud contamination, are plotted against salinity values (corrected for drill-mud content) in Figures 2a, 2b, and 2c. In each figure, a 'theoretical' seawater line is included, as well as a regression line, based on the 67 samples in Table 3. Due to the conservative nature of the cations and salinity in seawater, constant ratios would suggest that the pore water is similar to seawater. The regression line is based on reduced major axis regression statistics rather than using a least-squares regression approach. In cases where the independent variable has an uncertainty that is similar to the dependent variable, a least squares calculation is not appropriate (Till, 1974). Significant correlation coefficients result for the regression lines for all three figures. The theoretical sodium/salinity ratio for seawater is 306 while the regression estimate is 249 — a relative difference of 19%. Calcium and magnesium salinity ratios show regression ratios that have a relative difference of 7% and 6%, respectively, compared to seawater ratios. The sampling and analytical error is estimated to be on the order of 20%, and natural geological, microbiological, and geochemical processes can alter ion concentrations. Considering these factors, it is concluded that the salinity results and the cation/salinity regression ratios suggest that pore water in the gas hydrate section was originally seawater.

Magnesium questions

Ginsburg and Soloviev (1998, p. 141) presented results from the Caspian Sea gas hydrate studies where they discussed the distribution of magnesium in pore water. Salinities for these studies ranged from 14 ppt to 93 ppt, many of which were brine-rich solutions. The magnesium/salinity ratios ranged from 7 ppm/ppt to 17 ppm/ppt and tended to be lower in gas-hydrate-bearing samples. These ratios also tended to decrease with depth at a given location, suggesting that magnesium uptake by natural geological processes was occurring, as is often seen for magnesium in the Ocean Drilling Program data for both gas-hydrate-bearing and non-gas-hydrate-bearing samples. Ocean Drilling Program leg 164 magnesium/salinity ratios tended to be less than 15 ppm/ppt where depth below seafloor was more than 100 m (Paull et al., 1996).
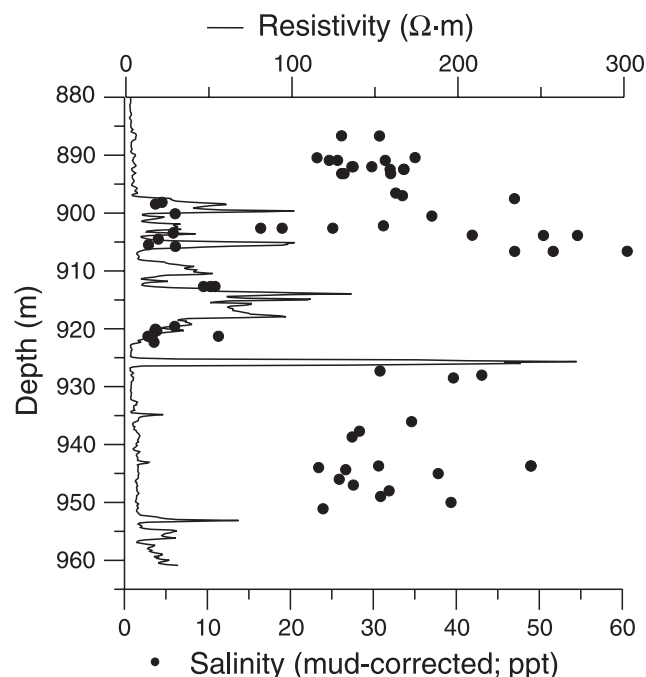

Figure 2.

a) *Sodium concentration versus salinity (corrected for drill-mud contamination);* **b)** *Calcium concentration versus salinity (corrected for drill-mud contamination)* **c)** *Magnesium concentration versus salinity (corrected for drill-mud contamination)*
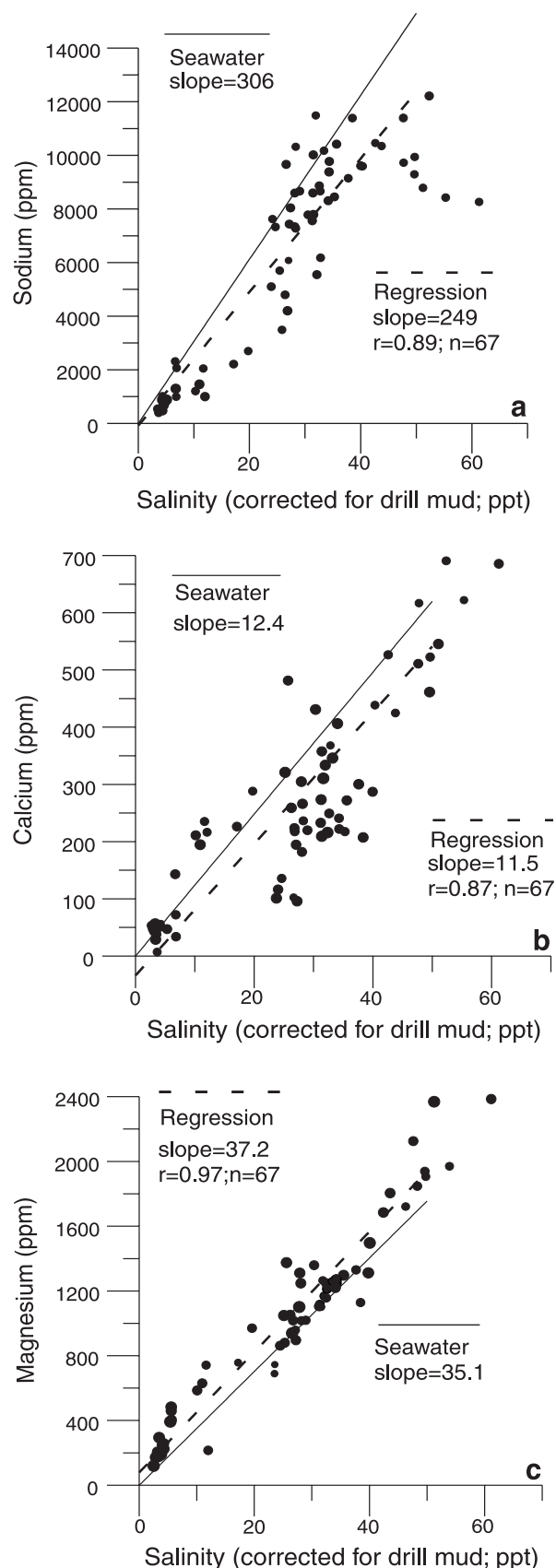
Magnesium/salinity ratios from the gas hydrate section at Mallik 2L-38 well averaged 38 ppm/ppt in pore water from non-gas-hydrate-bearing sediment, and 59 ppm/ppt for gas-hydrate-bearing samples. The magnesium/salinity ratios correlated to a highly significant degree with the presence of gas hydrate (Table 5), displaying values exceeding 50 ppm/ppt in many of the samples where gas hydrate was present (Table 3). It is concluded that the magnesium/salinity ratio was enhanced in gas-hydrate-bearing samples. The mechanism for this enrichment is unexplained. It is possible that the low-salinity solutions after gas hydrate dissociated encouraged the release of magnesium from surrounding sediments.

Downhole distributions

A reliable downhole log routinely used to indicate the presence of gas hydrate is resistivity (Collett et al., 1999). In Table 5, resistivity results correlated to a significant degree with other gas hydrate indicators (salinity, temperature, grain size, methane). The resistivity data is collected at a higher depth resolution than discrete sediment samples, thus providing a 'continuous' record of gas hydrate occurrence. Figure 3 contains the resistivity data plotted with downhole depth in the gas hydrate section. Included in this figure is pore-water salinity data for the 67 samples retrieved from this section. Clearly, pore-water salinities tend to be significantly lower in the higher resistivity region. What is also obvious is the trend for salinities to increase in non-gas-hydrate-bearing samples from a depth of 890 m to 907 m. Thin lenses of less

permeable, non-gas-hydrate-bearing, finer grained sediment are interspersed with coarser, gas-hydrate-bearing sediments. The thin lenses without gas hydrate contain higher salt concentrations that increase from about 30 ppt at 890 m to over 60 ppt at 907 m. As gas hydrate forms in the coarse-grained sediment layers, salt is expelled from the original pore water, which increases salinities in the non-gas-hydrate-bearing sections. Over time, some of the excess salt will diffuse to surrounding sediments with lower salinities provided that sediment porosity allows for this transport.

Estimating gas hydrate content

When the starting salinity of pore water and the salinity of pore water from dissociated gas hydrate is known, a calculation can be done to estimate the gas hydrate content in a sediment sample. Assuming that the gas hydrate occurs in spaces between sediment particles, and the bulk sediment porosity is known, another calculation can be made to estimate what fraction of the pore space contained gas hydrate. In the case of Mallik 2L-38 samples, the starting salinity of pore water before gas hydrate formed is not known, however from pore-water samples collected from non-gas-hydrate-bearing samples in the section, it appears that an average salinity is 34.5 ppt, and can reach 60.6 ppt. Assuming that the salinity of frozen water in gas hydrate is 0–2 ppt, it can be calculated what fraction of the water in a sample was frozen water in the form of gas hydrate, and what fraction was seawater with a salinity of 34.5 ppt. The average salinity for gas hydrated samples was 7.6 ppt (Table 4). In order to get this salinity, 22% of the water in this sample would come from water with 34.5 ppt, and 78% would therefore come from gas hydrate water with 0 ppt. At the other extreme, if the unfrozen water mixed in the gas hydrate sample had an enriched salinity of 60.6 ppt, a resulting mixture with 7.6 ppt salinity would result if 10% of the mixture was 60.6 ppt and 90% of the mixture came from frozen water with 2 ppt salinity.

It is estimated, to one significant figure, that gas hydrate filled 80–90 % of the pore space on average. Calculations from resistivity measurements (Collett et al., 1999), visual observations (Dallimore et al., 1999), and gas yields from dissociating gas hydrate (Dallimore et al., 1999) suggest that gas hydrate filled 50–90% of the pore space in many of the samples. These results can be compared to other estimates of gas hydrate recovered from various places. For example, Ginsburg et al. (1993) and Soloviev et al. (1994) found on the order of 40–90% of the pore space filled with gas hydrate in samples collected from the Okhotsk Sea when a salinity decrease of 20–60% was found. The recent work on the Blake Ridge during Ocean Drilling Program leg 164 showed gas hydrate contents on the order of 5% of the pore volume for a salinity decrease on the order of 5% (Paull et al., 1996). Ginsburg and Soloviev (1998, p. 156) provided a summary of 29 field programs where gas hydrate was thought to occur, where average salinity decreases in gas hydrated samples were 20%. The Mallik 2L-38 results show that salinities decreased by an average of 78% in the gas-hydrate-bearing samples which are among the highest numbers reported for gas hydrate freshening of pore water.

Figure 3. *Depth versus resistivity log and pore-water salinity.*

CONCLUSIONS

Geochemical pore-water salinity from the JAPEX/JNOC/ GSC Mallik 2L-38 gas hydrate research well indicate the occurrence of gas hydrate in intermittent zones from 898 m to 923 m downhole, agreeing with a number of independent measurements that can be used to identify gas hydrate zones. Pore water from gas-hydrate-bearing samples was an average of 78% fresher than pore water from non-gas-hydrate-bearing samples. This degree of freshening is among the highest reported in the scientific literature. It suggests that up to 90% of the pore space in the gas-hydrate-bearing sediment was filled with methane hydrate. Contamination from drill mud increased the salinity of pore water by an average of 2 ppt.

ACKNOWLEDGMENTS

REFERENCES

Collett, T.S., Lewis, R., Dallimore, S.R., Lee, M.W., and Mroz, T.H.
1999:   Detailed evaluation of gas hydrate resevoir properties using JAPEX/JNOC/GSC Mallik 2L-38 gas hydrate research well downhole well-log displays; *in* Scientific Results from JAPEX/JNOC/ GSC Mallik 2L-38 Gas Hydrate Research Well, Mackenzie Delta, Northwest Territories, Canada, (ed.) S.R. Dallimore, T. Uchida, and T.S. Collett; Geological Survey of Canada, Bulletin 544.

Cranston, R.E.
1991a: Gas hydrate experiments in the Okhotsk/Japan seas; Geological Survey of Canada, Open File 2446, 103 p.
1991b: Testing a higher resolution interstitial-water method for the Ocean Drilling Program; Proceedings of the Ocean Drilling Program, Scientific Results, (ed.) J. Barron and B. Larsen; v. 119, Ocean Drilling Program College Station, Texas, p. 903–931.

Cranston, R.E. and Standing, P.D.
1992:   Geochemical and sedimentological results from sediment cores collected in the Okhotsk/Japan seas; Geological Survey of Canada, Open File 2520, 67 p.

Cranston, R.E., Ginsburg, G.D., Soloviev, V.A., and Lorenson, T.D.
1994:   Gas venting and hydrate deposits in the Okhotsk Sea; Bulletin of the Geological Society of Denmark, Copenhagen, v. 41, p. 80–85.

Dallimore, S.R., Collett, T.S., and Uchida, T.
1999:   Overview of science program, JAPEX/JNOC/GSC Mallik 2L-38 gas hydrate research well; *in* Scientific Results from JAPEX/JNOC/ GSC Mallik 2L-38 Gas Hydrate Research Well, Mackenzie Delta, Northwest Territories, Canada, (ed.) S.R. Dallimore, T. Uchida, and T.S. Collett; Geological Survey of Canada, Bulletin 544.

Ginsburg, G.D. and Soloviev, V.A.
1998:   Submarine Gas Hydrates; VNIIOkeangeologia, 1 Angliyski prospekt, 190121 St. Petersburg, Russia, 216 p (translated and edited by V.L. Ivanov).

Ginsburg, G.D., Soloviev, V.A., Cranston, R.E., Lorenson, T.D., and Kvenvolden, K.A.
1993:   Gas hydrates from the continental slope, offshore Sakhalin Island, Okhotsk Sea; Geo-Marine Letters, v. 13, p. 41–48.

Jenner, K.A., Dallimore, S.R., Clark, I.D., Paré, D., and Medioli, B.E.
1999:   Sedimentology of gas hydrate host strata from the JAPEX/JNOC/ GSC Mallik 2L-38 gas hydrate research well; *in* Scientific Results from JAPEX/JNOC/GSC Mallik 2L-38 Gas Hydrate Research Well, Mackenzie Delta, Northwest Territories, Canada, (ed.) S.R. Dallimore, T. Uchida, and T.S. Collett; Geological Survey of Canada, Bulletin 544.

Mann, R. and Gieskes, J.M.
1975:   Interstitial water studies, Leg 28; *in* Initial Reports of the Deep Sea Drilling Project, (ed.) D.E. Hayes and L.A. Frakes; United States Government Printing Office, v. 28, p. 805–814.

Ohara, T., Dallimore, S.R., and Fercho, E.
1999:   Drilling operations, JAPEX/JNOC/GSC Mallik 2L-38 gas hydrate research well; *in* Scientific Results from JAPEX/JNOC/GSC Mallik 2L-38 Gas Hydrate Research Well, Mackenzie Delta, Northwest Territories, Canada, (ed.) S.R. Dallimore, T. Uchida, and T.S. Collett; Geological Survey of Canada, Bulletin 544.

Paull, C.K. et al.
1996:   Proceedings of the Ocean Drilling Program, Initial Reports; v. 164, Ocean Drilling Program, College Station, Texas, p. 315–316.

Solorzano, L.
1969:   Determination of ammonia in natural waters by phenolhypochlorite method; Limnology and Oceanography, v. 14, p. 799–801.

Soloviev, V.A., Ginsburg, G.D., Douglas, W.C., Cranston, R., Lorenson, T., Alekseev, I.A., Baranova, N.S., Ivanova, G.A., Kazazaev, V.P., Lobkov, V.A., Mashirov, Iu.G., Natorkhin, M.I., Obzhirov, A.I., and Titaev, B.F.
1994:   Gas hydrates of the Okhotsk Sea from the results of Leg 21 of R/V Petr Antropov, Otechestvennaya Geologia, v. 2, p. 10–17 (in Russian).

Strickland, J.D.H. and Parson, T.R.
1968:   A Practical Handbook of Seawater Analyses; Fisheries Research Board of Canada, Bulletin 167, 310 p.

Till, R.
1974:   Statistical Methods for the Earth Scientist; John Wiley & Sons, New York, New York, 154 p.

Wright, J.F., Taylor, A.E., Dallimore, S.R., and Nixon, F.M.
1999:   Estimating in situ gas hydrate saturation from core temperature observations, JAPEX/JNOC/GSC Mallik 2L-38 gas hydrate research well; *in* Scientific Results from JAPEX/JNOC/GSC Mallik 2L-38 Gas Hydrate Research Well, Mackenzie Delta, Northwest Territories, Canada, (ed.) S.R. Dallimore, T. Uchida, and T.S. Collett; Geological Survey of Canada, Bulletin 544.